International Journal of Fatigue 124 (2019) 361–370

Contents lists available at ScienceDirect

International Journal of Fatigue

journal homepage: www.elsevier.com/locate/ijfatigue

Characterization of cracks formed in large flat-on-flat fretting contact

Janne Juoksukangas[a,*], Verner Nurmi[a], Jouko Hintikka[c,1], Minnamari Vippola[b], Arto Lehtovaara[a], Antti Mäntylä[c], Joona Vaara[c], Tero Frondelius[c,d]

[a] Tribology and Machine Elements, Materials Science and Environmental Engineering, Faculty of Engineering and Natural Sciences, P.O. Box 589, 33014 Tampere University, Tampere, Finland
[b] Materials Characterization, Materials Science and Environmental Engineering, Faculty of Engineering and Natural Sciences, P.O. Box 589, 33014 Tampere University, Tampere, Finland
[c] R&D and Engineering, Wärtsilä, P.O. Box 244, 65101 Vaasa, Finland
[d] University of Oulu, Erkki Koiso-Kanttilan katu 1, 90014 Oulu, Finland

ARTICLE INFO

Keywords:
Fretting fatigue
Damage
Crack formation
Cracks
Microscopy

ABSTRACT

Fretting fatigue may lead to severe damage in machines. Adhesive material transfer spots in millimeter scale have previously been observed on fretted surfaces, which have been related to cracking. In this study, fretting-induced cracks formed in a large annular flat-on-flat contact are characterized. Optical and scanning electron microscopy of the fretting scar cross-section samples of self-mated quenched and tempered steel specimens revealed severe cracking and deformed microstructure. Two major cracks typically formed around an adhesion spot, which propagated at an oblique angle, regardless of the test parameters used. Millimeter-scale cracks were observed already within a few thousand loading cycles.

1. Introduction

Micrometer-level relative movement between contacts under normal loading may lead to fretting fatigue and severe damage in machine components. Cyclic fretting movement causes surface degradation and wear and promotes crack nucleation. Cracks may nucleate even at relatively low nominal cyclic stress levels. It is difficult to observe cracks that propagate inside contacts, which makes fretting an especially dangerous damage mechanism. Although many variables affect fretting, slip, coefficient of friction (COF) and normal load are typically considered as the most important [1].

The magnitude of slip in fretting is typically from a few micrometers up to some hundreds of micrometers. In gross sliding, the entire nominal contact area is slipping and in partial slip, certain areas are stuck while the rest of the contact is slipping. As discussed widely in the literature, gross sliding typically results in surface damage and wear. Such damage and wear is minimized in completely stuck contact without slip between the surfaces. Further, from a cracking point of view, the partial or mixed slip regime is typically regarded as the most dangerous, as cracks are known to form readily [2–4]. The COF can reach high values in fretting experiments in gross sliding conditions. Cyclic slip wears off oxide and contamination films leading to an initial increase in COF. After the initial increase, the COF typically stabilizes at values in the range of 0.8–0.9; though some material such as QT produced 'friction peak' where COF can reach values up to around 1.5 [5,6], followed by a decrease and stabilization at values in the range of 0.8–0.9 similar to most materials. In addition, COF can have a distribution along the contact interface [7]. High COF can be a prerequisite for crack nucleation since it is needed to cause the high contact shear stresses that promote crack nucleation [8].

Fretting is known to have a major role in nucleating cracks. It tends to nucleate multiple cracks, which may coalesce [9], propagate or arrest [10]. Apart from the influence of contact stresses, crack propagation is made possible due to bulk loading. Although the principles of fracture mechanics concepts have been employed to study long crack propagation, the fretting crack nucleation mechanism is still not fully understood. Fretting contact induced stresses affect the surface and its vicinity, and this is typically the place for crack nucleation. Severe plastic deformation can exist in fretting contacts [11] and at the crack nucleation site [11–13]. Contact loading may orientate grains and decrease their size and flatten them [14,15]. It is usually reported that most of the fretting fatigue life is spent in crack propagation. Cross-section samples have revealed cracking within only a few hundreds [16] or thousands of fretting cycles, even without bulk loading [4]. Typically, cracks nucleate at surface points where stresses are highest, such as at the edges of the contact [10,13,17–20], close to stick-slip

* Corresponding author.
E-mail address: janne.juoksukangas@tuni.fi (J. Juoksukangas).
[1] Formerly: Tribology and Machine Elements, Laboratory of Materials Science, Tampere University of Technology, P.O. Box 589, 33101 Tampere, Finland.

https://doi.org/10.1016/j.ijfatigue.2019.03.004
Received 6 December 2018; Received in revised form 1 March 2019; Accepted 3 March 2019
Available online 04 March 2019

boundary [17,21,22] or at adhesive cold weld junctions [23]. Fretting-induced cracks typically propagate close to the contact interface at an some oblique angle [13,24], like 30 [4] or 45 degrees [24], due to the shear loading induced by fretting. Then, outside the influence of contact loads, the crack turns to a direction corresponding to mode I stress intensity.

Fretting fatigue tests with quenched and tempered steel (as used in [5]) have been done using a complete contact fretting test device [25–27] and also a bolted joint setup [28]. A marked decrease in fatigue life has been observed due to fretting. Adhesive material transfer spots (cold welding) including visible cracks on the contact surface have been observed in large flat-on-flat contacts [5,28], indicating that material transfer spots carry normal and tangential forces which will introduce stress localizations. These spots have been related to non-Coulomb friction [29,30], where friction force increases during a loading cycle as the reversing point is approached, resulting in a hook-shaped form in measured hysteresis loops.

Fretting fatigue studies relating to quenched and tempered steels are somewhat scarce in the literature because fretting fatigue is mostly studied using aluminum and titanium alloys. However, quenched and tempered steels are widely used in fatigue prone machine parts in mechanical engineering. Further, mostly used Hertzian type fretting contacts with some geometric form (e.g. cylinder against flat surface) leads to specific distributions of contact tractions and slip. In addition, the contact size is typically relatively small, leading to fretting fatigue "size effect" [31] and also normal pressure may be high. In Hertzian-type contact the stresses are sufficiently high that fatigue failure may be predicted using multiaxial failure criteria [32,33]. However, in certain types of flat-on-flat contacts [28], where such macroscopic geometry-induced localization of the stresses does not occur, the initiation of cracks and fretting damage has been shown to occur even when these fatigue criteria do not predict failure. However, in practice fretting may prevail in large flat-on-flat contact [34,35] under a modest normal pressure. An annular flat-on-flat surface produces quite even contact tractions and sliding distribution, as shown in [5], with no geometrical edges in the sliding direction and makes it possible to use relatively low normal pressures.

The material alterations in the specimens analyzed here have been studied previously [36] using cross-sections and some of the test results have been published, mainly in relation to frictional behavior and surface degradation [5,29,37,38]. Microstructure at the adhesion spots was significantly plastically deformed [36]. Three degradation layers were found at the adhesion spots and their immediate vicinity; the general deformation layer, the tribologically transformed structure (TTS) and the third body layer. The very hard TTS itself contains numerous cracks, as it has been under excessive plastic deformation. These cracks are oriented at an angle of approximately 45 degrees to the contact surface. The objective of this study was to characterize fretting cracks formed in a wide variety of operating and running conditions in the large-scale flat-on-flat surfaces using quenched and tempered steel specimens.

2. Methods

2.1. Test device

All experimental fretting tests were carried out using an annular flat-on-flat fretting test device, which is described comprehensively by Hintikka et al. [5]. Two axisymmetric fretting specimens are under normal load with one specimen rotated in oscillating manner, while the second is fixed, leading to slip and fretting between the specimens. The specimens clamped together create a large annular flat-on-flat contact with no edges in the sliding direction and have a nominal contact area of 314 mm^2. Fig. 1 presents the test specimen and cross-sections of the two specimens and their holders, contact surface description and normal pressure distribution.

The annular flat-on-flat contact has somewhat linear normal pressure distribution (Fig. 1C) which deviates radially a maximum of about 18% from the average normal pressure value, being highest at the inner annulus (numerical analysis in [37]). The normal load (nominal normal pressure), as well as the rotation (sliding amplitude) can be adjusted continuously. These are also measured together with the frictional torque during the entire experiment. From these measurements, the COF is determined in gross sliding conditions. Even though rotation is measured some distance away from the contact, rotation and sliding amplitude at the contact is obtained and presented by ruling out the specimen elastic deformation. The rotation is displacement-controlled by an actuator with feedback from the measured signal.

2.2. Material and test specimens

The material used in the tests was quenched and tempered steel EN 10083-1-34CrNiMo6 + QT having a totally tempered martensitic microstructure. Table 1 shows the chemical composition of the used steel.

The composition was measured with energy dispersive spectrometry of a scanning electron microscope, which does not allow accurate quantification of carbon. For this reason, the amount of carbon is not presented in Table 1. The yield strength of the material is 994 MPa and the ultimate tensile strength 1075 MPa. A plain fatigue limit of 517 MPa has been measured for the same steel [25]. The surface roughness (*Sa*) of the ground specimens varied between 0.20 and 0.32 µm. Before fretting testing, the specimens were cleaned in an ultrasonic device with solvent.

2.3. Test procedure

Most of the analyzed tests were carried out in gross sliding regime having sliding amplitudes of some dozens of micrometers. In gross sliding condition, the contact area is experiencing sliding in its entirety. The running condition is determined using ideal contact conditions. Tests below fully developed friction load (with small sliding amplitude) were also carried out. In these tests, only limited amount of friction was utilized. In addition, a few short length tests in gross sliding regime were made. In all tests, the nominal normal pressure was between 10 and 50 MPa and the sliding amplitude from close to zero up to 65 µm. The normal load remained constant in the individual tests. The normal pressure distribution was checked and adjusted before each test using a pressure sensitive film. Elastic deformations of the specimen and test device have been removed in these reported sliding amplitude values.

The fretting loading (rotational) frequency was 40 Hz. The rotation amplitude was ramped up during the first 400 loading cycles and correspondingly ramped down during 100 loading cycles at the end of every test. The main test duration was three million loading cycles but short length tests in gross sliding regime with 100, 1000 and 10,000 loading cycles (not counting ramping cycles with lower sliding amplitude) were also carried out. The temperature and humidity in the lab were 19–25 °C and 14–24% in the short length tests and in the other tests between 25 and 30 °C and 22–44%, respectively. The test matrix is shown in Table 2, presenting the section where the tests in question can be found, as well as the series name, the amount of loading cycles N_{LC}, the nominal normal pressure p and the sliding amplitude u_a.

2.4. Characterization

The characterization methods are described in more detail by Nurmi et al. [36]. In short, the specimens for cross-sections were cleaned after fretting testing with acid detergent. At this point Leica MZ75 optical microscope was used to image the contact surface. Fig. 2 shows a fretting contact surface and the location of a cross section that was made. The cross-section samples were made in parallel with the sliding direction from the visually determined most severely degraded scars, i.e., adhesion spots, as shown in Fig. 2. It was assumed that the longest

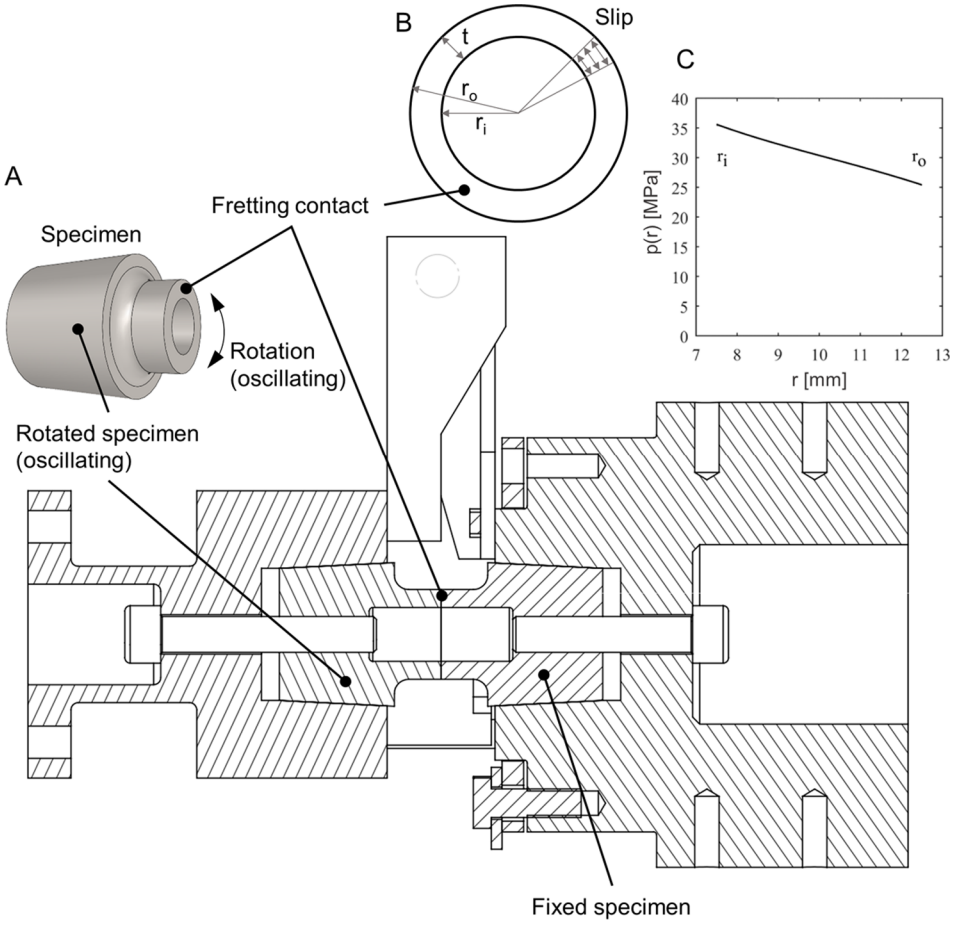

Fig. 1. Test specimen and a cross-section of the two specimens in contact and their holders (A) in the used annular flat-on-flat fretting test device, contact surface (B) and normal pressure distribution (C).

Table 1
Chemical composition of the used material.

Element	Si	Mo	Cr	Mn	Fe	Ni	Total
Wt %	0.3	0.6	1.3	0.8	95.8	1.3	100.0

cracks would be found here. The cutting was performed approximately at the centerline of an adhesion spot. One cross-section covered roughly 13% of the circumference of the specimen. After grinding, polishing and etching, Leica DM 2500 M optical microscope and Philips XL 30 scanning electron microscope (SEM) were used to document the cross-sections. Crack lengths were determined from microscope images using ImageJ software.

3. Results

Fretting damage on the contact surfaces was observed in every test. The most severe fretting scars in terms of damaged area were observed in the full length gross sliding tests, where in some tests the whole specimen nominal area was damaged. In addition, the longer the test duration, the larger the area of fretting damage was. Fig. 3 shows the effect of different operating parameters on surface damage.

The total amount of loading cycles was 3×10^6 in all cases presented in Fig. 3. The higher the sliding amplitude, the larger the area of fretting damage (A, B, D). Normal pressure has a similar effect. The higher the normal pressure, the larger is the area of fretting damage (C, D). Most of the tests produced millimeter-scale adhesion spots, as shown in the surfaces in Fig. 3. Adhesion spots were already observed with a normal pressure of 10 MPa (C). Inspection of surfaces revealed protrusions and dents, which are evidence of adhesive material transfer [5]. During the initial stage of the tests, adhesive wear and material transfer dominate, while debris creation changes the major wear behavior from adhesive to abrasive wear. Visible cracks on the contact surface were found in many gross sliding samples by using optical microscopy.

Table 2
The test matrix.

Section	Test series name	Loading cycles N_{LC}	Normal pressure p [MPa]	Sliding amplitude u_a [μm]
3.1	Full length gross sliding	3×10^6	10, 30	5, 20, 35, 50, 65
3.1	Full length gross sliding	3×10^6	50	20, 35, 50
3.2	Short length gross sliding	100, 1000, 10,000*	30	35
3.3	Below fully developed friction	3×10^6	30	≤ 3.5

* Not counting ramping cycles (500 in total).

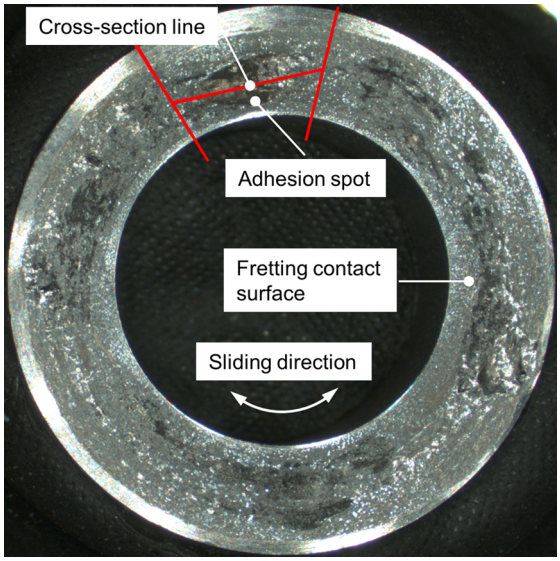

Fig. 2. Cutting position of a test specimen.

3.1. Full length gross sliding tests

In the full length gross sliding tests with the amount of loading cycles of 3×10^6, the sliding amplitude ranged between 5 and 65 μm and the nominal normal pressure between 10 and 50 MPa. In the results presented here, the COF is calculated from the measured maximum frictional torque amplitude during a loading cycle and the normal pressure distribution [5], representing the maximum COF during one loading cycle. In all gross sliding tests, the COF peaked at the beginning of the tests with the maximum COF of about 1.4 and the stabilized, steady state COF after decrease was about 0.8.

Overall, clear and extensive cracking was observed from the cross-sections. Under the most degraded areas, adhesion spots, the longest cracks appeared as pairs, as shown in Fig. 4. This can be explained by the cyclic and reversing loading of the fretting contact. The crack pair is typical for all gross sliding tests analyzed, but also for some tests where sliding amplitude was much less (Section 3.3). The focus of this study was these longest cracks created around adhesion spots, as seen in Fig. 4. The cracking of the TTS-layer has been studied earlier [36].

Major cracks nucleate at the surface, most likely at the edges of the adhesion spot, where local stress is expected to be high. However, no correlation could be made between visually measured adhesion spot size on the contact surface and crack dimensions (the distance between crack pairs). The obvious explanation is that the fretting scar is still evolving after the crack pair has been formed. Moreover, the determination of fretting scar features from the degraded contact surface is no easy task. Fig. 5 shows a more detailed view of a major crack in another specimen with sliding amplitude 35 μm and normal pressure 10 MPa. Cracks propagate at an oblique angle to the contact surface towards the base material. This is typical behavior and often found in the literature but in those cases cracks form often at the edges of the contact, whereas here a crack pair forms at nominally flat surfaces inside the contact.

As shown in the Fig. 5, the crack changes its orientation during propagation. Close to the contact surface, the angle to the contact surface is quite small but after a few dozen micrometers, the angle gets bigger and stays quite constant thereafter. In the full length gross sliding specimens, multiple smaller and arrested cracks of some dozens of micrometers in length having a slight angle were observed close to the contact surface. These might contribute to delamination and the creation of fretting debris. Most of the cracked area is also martensite. Significant plastic deformation can be observed at the adhesion spot between the crack pair. It seems that the crack size is limited to the size of the fretting induced plasticity region. Hardness is increased here by 50–70% compared to the base material and EBSD results also reveal severe plasticity [36]. From EBSD images it was observed that grains

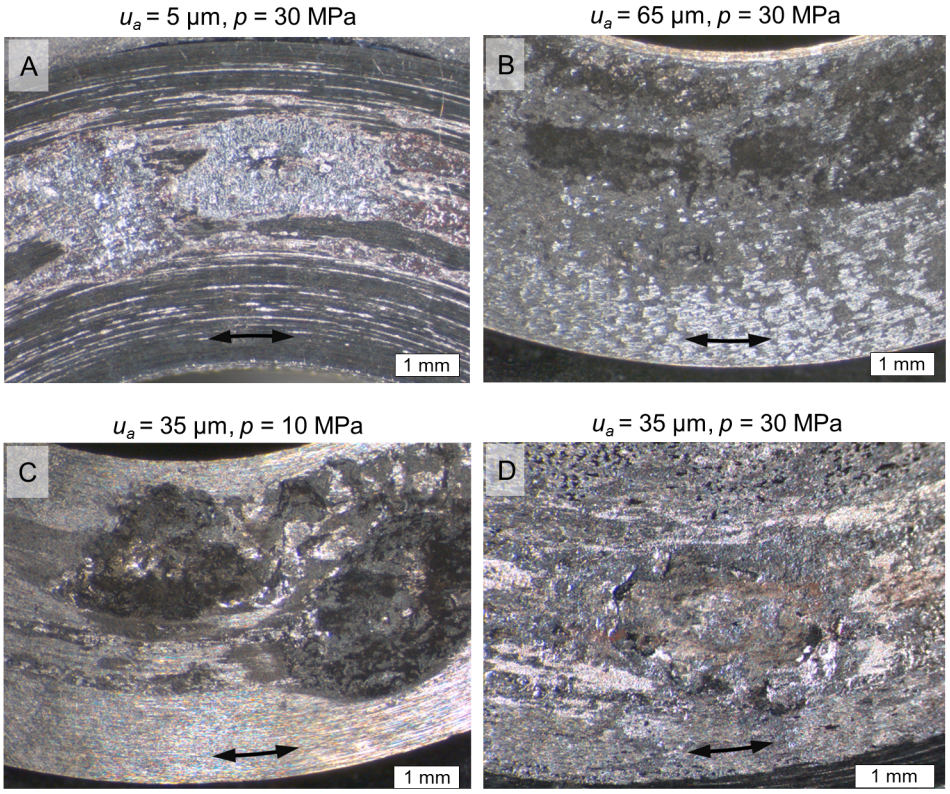

Fig. 3. Fretting scars of gross sliding specimens with different operating parameters, u_a is sliding amplitude and p is normal pressure. Total amount of loading cycles was 3×10^6 in each case. The arrows show the sliding direction.

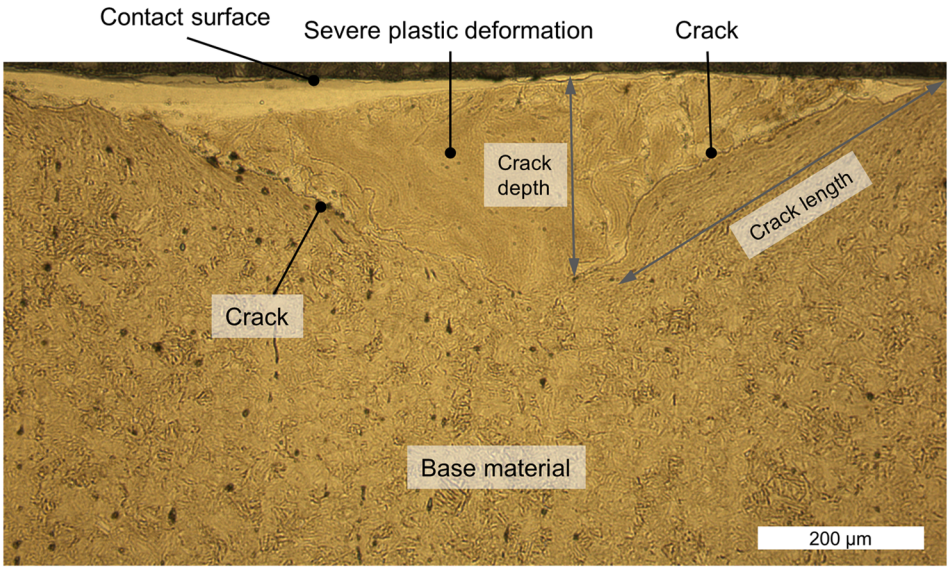

Fig. 4. Crack pair in a gross sliding test, $u_a = 20\,\mu m$ and $p = 30\,MPa$.

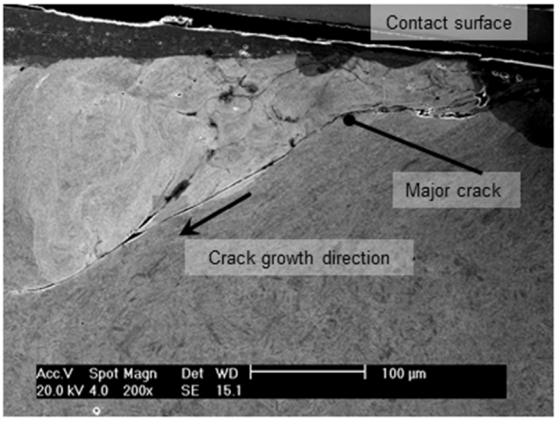

Fig. 5. Major crack details in a gross sliding test, $u_a = 35\,\mu m$ and $p = 10\,MPa$.

had flattened and those near the cracks had orientated in the same direction as the cracks. Plastic deformation was less severe near the crack ends and in the area between two crack ends.

Crack lengths and depths were measured from the microscopic images of cross-sections. The longest crack lengths with various sliding amplitudes and normal pressures are shown in Fig. 6.

Crack lengths clearly increase as the sliding amplitude is increased, regardless of the normal pressure, up to the sliding amplitude of 35 µm. At higher sliding amplitudes, 10 MPa (sliding amplitude 50 µm) and 30 MPa (sliding amplitude 65 µm) values show much smaller crack lengths, but the rest of the points still support the increasing trend. In addition, the average value taking into account all normal pressures still suggests the increasing trend up to the sliding amplitude of 50 µm. The relation between normal pressure and crack length is less obvious, but the average of each normal pressure value suggests that crack length is increased with the normal pressure. However, these can be within statistical scatter due to the low number of tests. With the lowest values of sliding amplitude, the crack lengths measured are some dozens of micrometers, which is within the size scale of the material grain size. The longest crack lengths were well over a millimeter, which are notably over the grain size. Thus, the principles of fracture mechanics may be applied.

Fig. 7 shows the correlation between crack length and crack depth. Correspondingly to crack length, the crack depth is the deepest measured within one cross-section. The depths varied from a few micrometers up to a little over half a millimeter.

The crack length and crack depth have a linear correlation. The average angle for crack propagation to the contact surface is 26.2 degrees determined from these results. This angle is approximately the same regardless of test parameters. The distance between crack pairs at the nucleation point on the surface was measured from the cross-sections and is presented in Fig. 8. In some cases severe plastic deformation

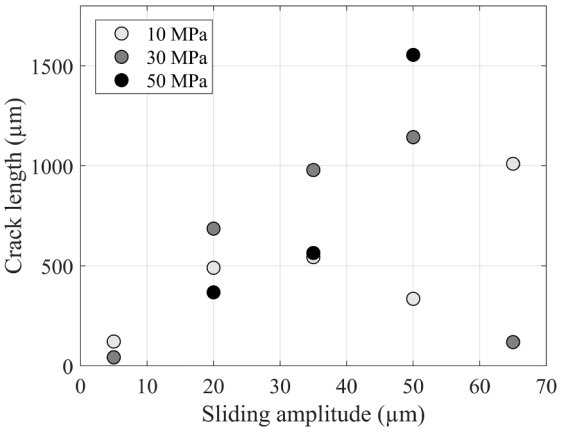

Fig. 6. Crack lengths with various sliding amplitudes and normal pressures.

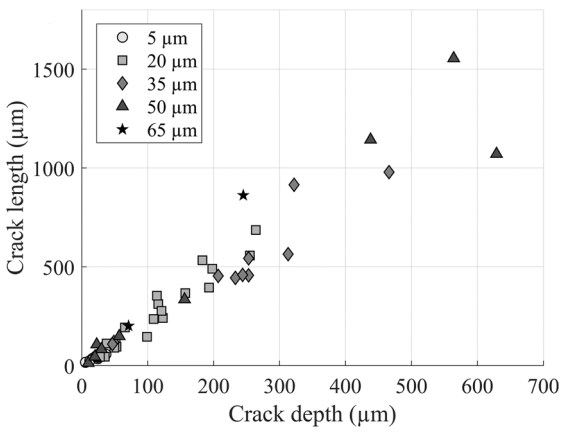

Fig. 7. Crack lengths in relation to crack depth with various sliding amplitudes.

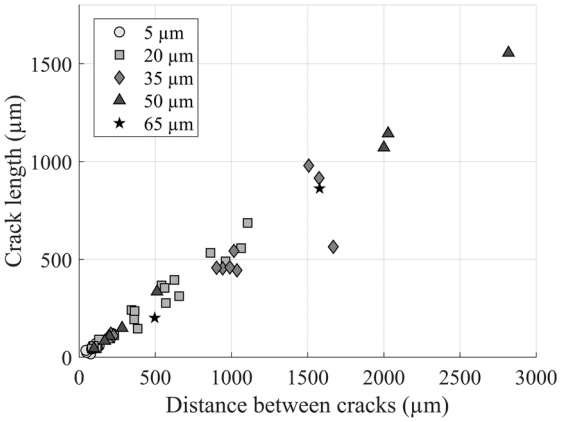

Fig. 8. Crack length as a function of distance between cracks at the nucleation point on the surface.

and wear debris at the crack nucleation site make it difficult to determine the crack nucleation point.

The wider the distance between a crack pair is, the longer the cracks are. Crack depth also correlates linearly with the distance between cracks. Crack length, depth and distance between a crack pair thus have a linear correlation with each other. Even if fretting test parameters and running conditions change, the relative crack geometry remains relatively constant. It seems that cracks nucleate at the edges of an adhesion spot (cold welding), in the same manner as at contact edges often reported in the literature. However, in this case adhesion spots and cracking occur between nominally flat surfaces without any macroscopic geometrical shape. As noted earlier, a gross sliding regime is typically considered as a regime producing surface damage and wear rather than cracking. However, these results revealed that significant cracking also occurred in nominally gross sliding samples.

One test specimen from a full length gross sliding test having sliding amplitude of 50 µm and normal pressure of 30 MPa was prepared for fracture surface inspection. As specimens do not completely crack in the test device, the fracture surface needs to be opened. First, a thin 1.5 mm section was cut from a chosen sample having an adhesion spot as big as possible. The section was torn open at the point of the adhesion spot, weakened by the crack. The fracture surface is shown in Fig. 9.

In (A), the fracture surface and a part of contact surface (fretting scar) is shown. The sliding direction and the crack growth direction are marked. Magnified images are shown on the right (B and C). Red boxes indicate the areas of the magnified images. The cracks approximately normal to the sliding direction may have been formed in the opening (tearing) process. The fracture surface close to the nucleation area (contact surface) does not clearly indicate fatigue, ductile or brittle fracture behavior. However, fatigue striations corresponding to cyclic fatigue crack growth were found after some propagation, as shown in (C). Interestingly, the measured crack growth rate from the striations is about 0.45 µm/cycle (at the location of the arrow in the figure), thus roughly corresponding to the value determined in the short length gross sliding tests (Section 3.2). Similar results have also been observed in the literature [39], where fatigue striations were observed at some distance from the actual nucleation site.

3.2. Short length gross sliding tests

Short length (interrupted) gross sliding tests were made to study early formation of fretting damage, crack formation and initial phases of crack propagation in more detail. Test durations were 100, 1000 and 10,000 loading cycles (not counting the ramping cycles at the beginning and at the end of the test). The sliding amplitude was 35 µm and normal pressure 30 MPa. Fig. 10 shows the COF curves during these tests and test lengths. The ramping cycles are marked with a solid gray area.

The COF increases markedly during the initial cycles having the peak value about 1.4, before it starts to decrease and stabilize. Approximately identical friction behavior is observed between short and full length gross sliding tests during the corresponding loading cycles and thus their comparison is relevant. Already in the 100 loading cycle case (total amount of 600 cycles due to the rampings), the COF has started to decrease after peaking. Thus, in all the reported tests here, the peak in friction has already occurred. Fig. 11 shows fretting scars and cracks at selected locations.

It can be clearly observed how the area of fretting damage on the surface increases during loading cycles. Adhesion spots form after only

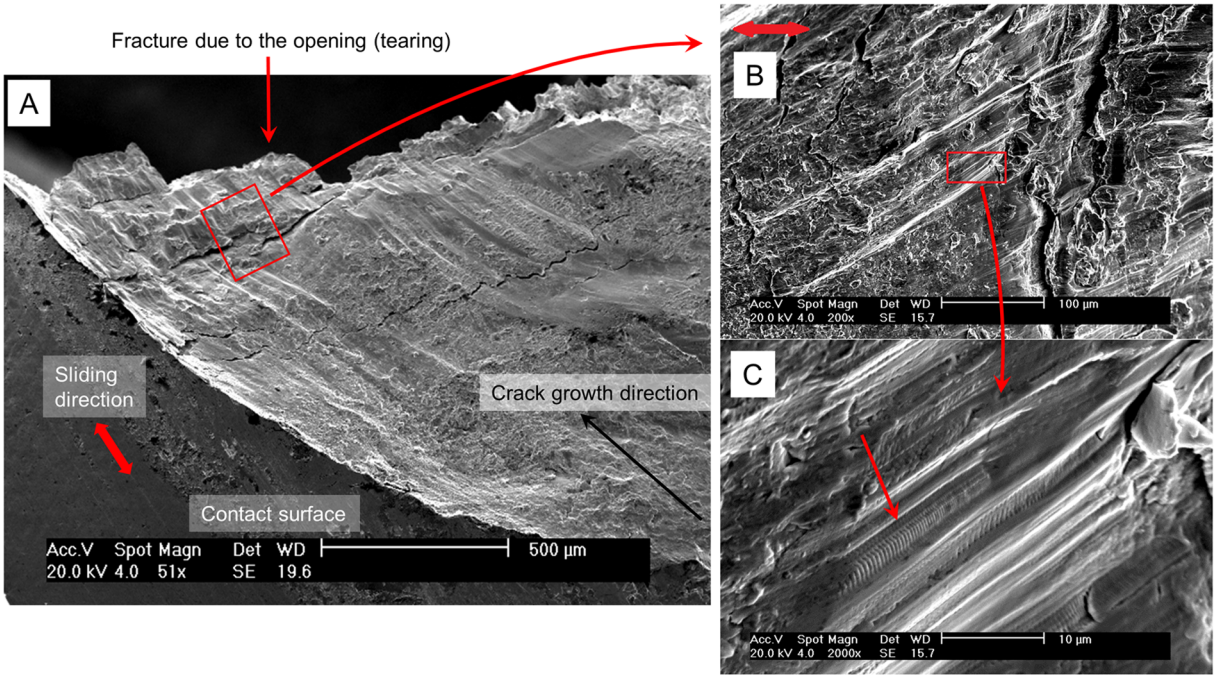

Fig. 9. Fracture surface of a fretting-induced crack. Note the different orientation between the figures at left and right.

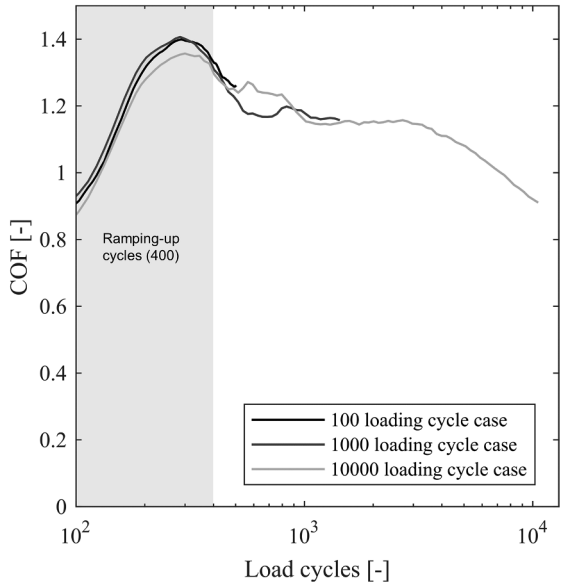

Fig. 10. Coefficient of friction during the short length tests, u_a = 35 μm and p = 30 MPa.

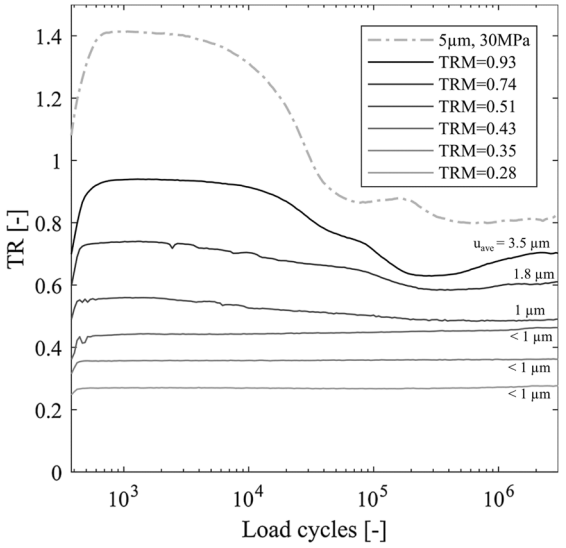

Fig. 12. Torque ratios of tests below fully developed friction and a gross sliding test with u_a = 5 μm and p = 30 MPa.

a small number of loading cycles. Noticeable tensile force was needed to pull specimens apart in some short length tests, which is a clear indication of adhesion and cold welding between the specimens. Already in the 100 loading cycle case plastic deformation and cracks were observed. The peculiar shape of the contact surface in the 100 loading cycle case may be due to the pulling-induced tension after the test. However, these cracks in short length tests were in average smaller than in full length tests. As cracks had already nucleated after a relatively small amount of loading cycles, it seems that cracks are caused by heavy overstressing [40]. A clear crack pair having individual lengths of hundreds of micrometers was formed within 1000 loading cycle case, and the crack dimensions were already at the same level as in the full length tests. Crack nucleation and propagation has therefore been rapid. Taking into account the ramping cycles of a test, the average crack growth rate can be almost 0.5 μm/cycle. In addition, the plasticity

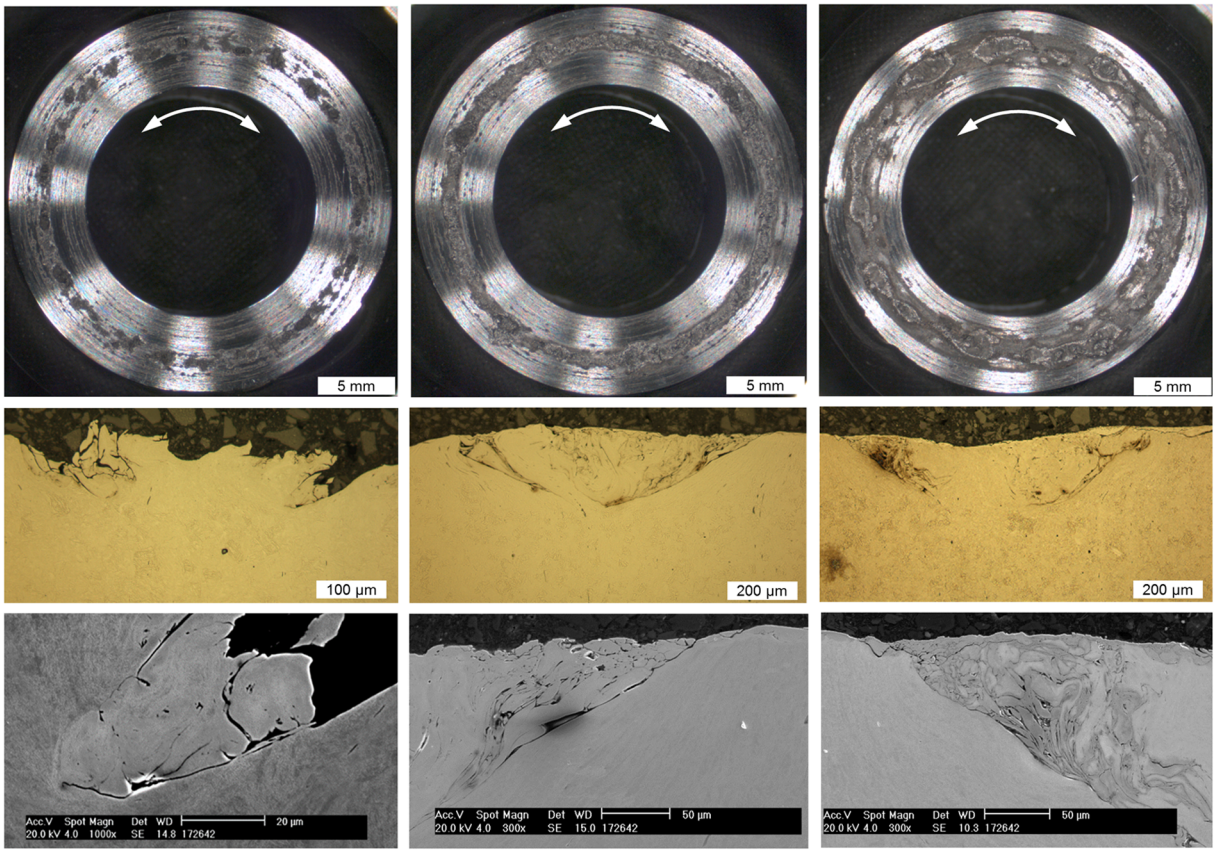

Fig. 11. Fretting contact surface (upper row), crack pair (middle row) and crack details (lower row) of short length tests. From left to right 100, 1000 and 10,000 loading cycle cases. The sliding direction is marked by white arrows.

region resembles the corresponding regime in the full duration tests.

3.3. Tests below fully developed friction

These tests were performed with load levels below fully developed friction [37,38], i.e., with limited utilization of friction, resulting in sliding amplitudes in the range of only a few micrometers. As COF is the coefficient of friction in gross sliding condition where all surface points are sliding, it cannot be used in stick and partial slip conditions. Therefore, torque ratio (*TR*) was used to analyze frictional properties instead of COF. *TR* is the ratio between tangential traction amplitude and normal traction, which corresponds to COF in gross sliding conditions [37] and is also valid in partial slip conditions. Fig. 12 shows the *TR* curves of these tests.

TRM is the maximum *TR* value observed during the test. Tests having *TRM* values 0.28, 0.35, 0.43, 0.51, 0.75 and 0.93 were analyzed. The normal pressure applied was 30 MPa. The maximum of average sliding amplitude u_{ave} during the tests is shown. The average sliding amplitude is determined from rotation amplitude and average radius of the specimen (10 mm). The rotation amplitude at the zero torque (during a cycle) is used to remove elastic deformations [37]. The average sliding amplitudes varied from close to zero up to 3.5 µm. For comparison, one gross sliding curve of a test having maximum and stabilized *TR* (COF) values of about 1.4 and 0.8, respectively, is presented. Fig. 13 shows fretting scars and SEM images from cross-sections of tests having *TRM* values of 0.35, 0.75 and 0.93.

Overall, these tests led to significantly less severe fretting damage and surface wear compared to the gross sliding tests (particularly full length gross sliding tests), especially when *TR* was small. The higher the *TR* value and sliding amplitude, the more severe the fretting scar was. With *TRM* = 0.93 (C), the fretting scar resembles the surface damage seen in gross sliding tests, though less severe. With small *TR* values and sliding amplitudes, crack pairs did not form, as shown in Fig. 13(A). Identification of micrometer-level cracks is challenging, and the cracks can be mistaken for material defects. These small cracks were not within the scope of this study. When *TRM* value was 0.93, in addition to the increased level of fretting-induced damage, a clear crack pair was formed, Fig. 13(C). In addition, crack length increases having lengths of dozens of micrometers. However, the cracks are still much shorter than the cracks in the gross sliding tests. According to the results, adequate utilization of friction and sufficiently large slippage are essential for cracks to form.

4. Discussion

The results show the great tendency of fretting to create cracks. Cross-sections were made focusing on the most severe looking fretting scar (adhesion spot). Multiple small cracks having dimensions of material grain size were observed close to the contact surface, which is typical in fretting, but mainly the observations were characteristics of two major cracks around the adhesion spot. The analysis of fretted surfaces by imaging may reveal cracks but a more precise way to find cracks is to use cross-section analysis. Almost in every analyzed test cracks of at least dozens of micrometers were observed, the biggest cracks being over a millimeter in length. The size of cracks increased linearly up to the sliding amplitude value of 35 µm, but after that, in some tests the size decreased as the sliding amplitude was increased. It may be that higher slip leads to increased wear that may play a role, since embryonic cracks can be worn off before propagating further, or higher slip may affect the contact adhesion response by means of

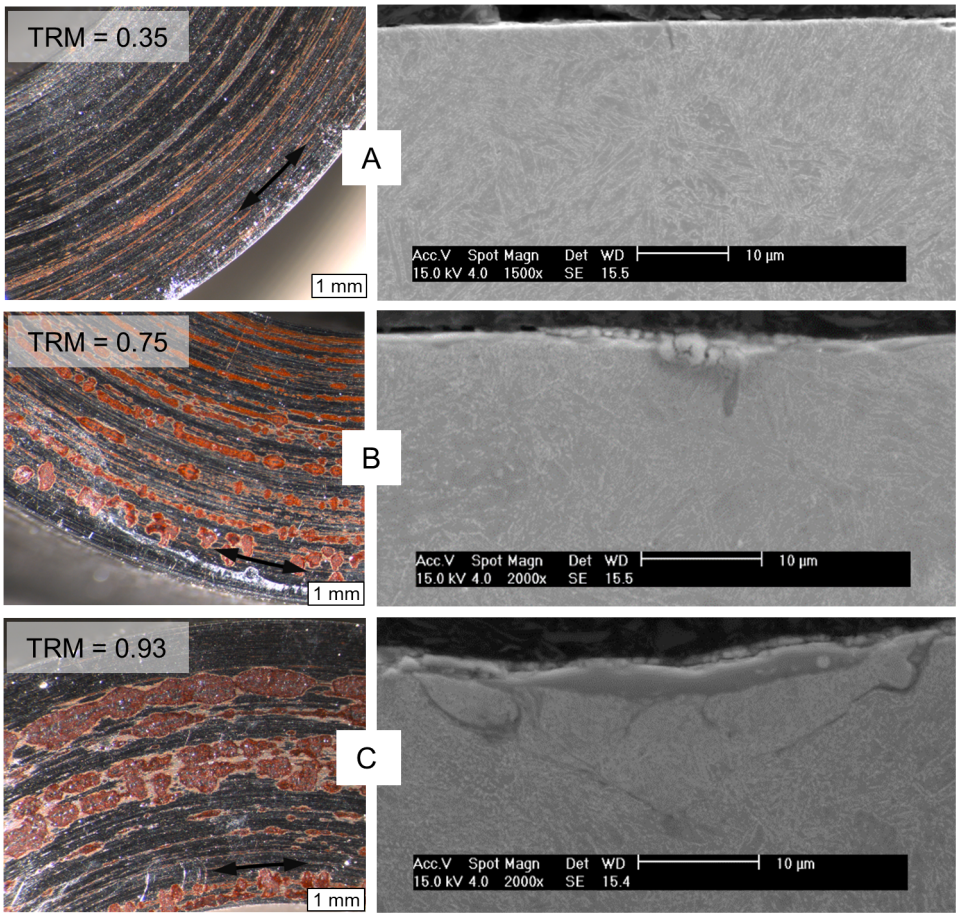

Fig. 13. Fretting scars and SEM images with TRM values 0.35 (A), 0.75 (B) and 0.93 (C). Sliding directions are shown by the black arrows.

shearing and/or fatigue of asperity tip junctions. According to the few short length tests, cracks form very early in the loading history, thus representing low cycle fatigue conditions rather than high cycle conditions. Broader study of this appears to be important further topic focusing, in particular, the relation between observed frictional behavior and crack forming.

The focus of this study was to study the formation of fretting-induced cracks whose formation and propagation is promoted by the contact stresses. Rather than the presence of a pre-existing flaw, cracking was due to damage accumulation because of the high local stresses induced by fretting. In a fretting contact, the stress state and slip should affect the nucleation of cracks, although further the growth in the propagation phase is determined by the conditions at the crack tip. In the majority of the measured cracks the lengths were multiple times longer than the grain size of the material, thus their behavior can be described by the principles of fracture mechanics. Severe plastic deformation and cracking were observed already with a nominal normal pressure of 10 MPa. Therefore, very high local loading conditions must exist at the adhesion spots that cannot be predicted using nominal loadings on the nominally flat-on-flat contact surfaces without considering microscale grain structure. The formation and localization of adhesion spots may be affected by minor deviations in manufacturing of flat surfaces or surface topography. The nominal stresses due to the frictional torque in the contact are some dozens of megapascals and are thus very low compared to the fatigue strength of the used steel (517 MPa), so cracks leading to complete specimen fracture was not expected. Obviously, if adequate cyclic bulk stress is applied, these cracks are expected to propagate.

Fig. 14 shows a schematic presentation of the evolution of the annular flat-on-flat fretting contact using quenched and tempered steel.

Initially the *Q/P* ratio (the ratio of tangential force amplitude to normal load), i.e. COF in gross sliding, increases due to the evolution of adhesion leading material transfer. Cracking may already be present at this point. At its peak, frictional behavior is highly non-Coulomb in nature due to tangential fretting scar interactions [29], as shown in the hook-shaped fretting loop, presenting the energy dissipated by the friction. Already at this point excessive plastic deformation and relatively big cracks were observed (Fig. 11, the short length tests), so crack nucleation has been relatively rapid. A tribologically transformed structure and third body layer have been observed to clearly develop within about 10 000 loading cycles [36]. The COF value decreases markedly from the peak value and stabilizes after some thousands or ten thousands of loading cycles. Non-Coulomb conditions are revealed, as shown by the rectangular-shaped fretting loop. Fretting wear produces oxidized debris that can be partly entrapped within the contact and partly ejected from the contact.

According to Hintikka et al. [37], the transition from partial slip to gross slip in this annular-type of flat-on-flat contact occurs with COF of 1.0 at average sliding amplitude of 0.5 μm. Experimental tests start with ramping up the rotation (sliding amplitude). Thus, at least at the very beginning of a test the contact is in partial slip conditions, but it will quickly move to gross sliding, when enough rotation is applied. In the majority of tests presented here, the gross sliding condition is prevailing. These ideal conditions were followed in this study. However, it is clear that the adhesion spots do not follow these ideal conditions. As a result, although contact is seemingly in gross sliding regime, it is likely that these local contact areas (adhesion spots) are stuck at least momentarily in the loading history, and therefore a local partial slip condition exists. It may also be possible that a localized high COF in adhesion spots results in similar type of crack pair shown here. Crack may nucleate at the boundary between the resulting stick and sliding regimes, as often reported in the literature in the partial slip conditions. However, it is emphasized that in those cases Hertzian contact is often used, whereas here a crack pair forms at nominally flat surfaces inside the contact. Regardless, the true behavior at the adhesion spots remains unknown and the determination of the local conditions at the adhesion spots for evaluating cracking behavior is important and warrants further study.

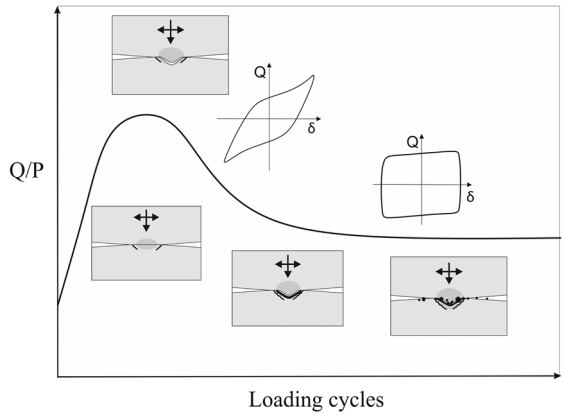

Fig. 14. Schematic presentation of the evolution of the fretting contact.

5. Conclusions

Fretting-induced crack formation was studied in large flat-on-flat contact by making cross-section samples from fretting scars. The material used was self-mated quenched and tempered steel 34CrNiMo6. Test specimens with different sliding amplitudes, nominal normal pressures, test lengths and loading conditions were analyzed. The following conclusions can be made:

- Annular flat-on-flat contact creates local adhesion spots which revealed significant fretting-induced cracking and plastic deformation, especially in tests having enough high sliding amplitude.
- The formation of cracks can be explained with local stress concentrations around the adhesion spots. Even the contact is nominally in gross sliding conditions, localized stick areas (adhesion spots) likely exist at least at some moment in the loading history.
- Mostly two major cracks with lengths at least of hundreds of micrometers were formed at an adhesion spot. The cracks nucleated on the surface and grew towards each other at an average crack angle to the contact surface of about 26 degrees, regardless of fretting test parameters. Smaller arrested cracks were also observed close to the contact surface.
- Linear correlation existed between crack length and the distance between the nucleation points between a crack pair.
- Clear cracking was observed when the maximum value of the ratio between tangential traction amplitude and normal traction during testing was larger than 0.8.
- Cracks seemed to form at the initial stages, as the thousand cycle test shows similar crack lengths as the full length tests of three million cycles.
- Cross-sections made from fretting scars are an efficient and precise way to study cracking and material degradation. Visual inspection of fretting damaged surface using optical microscopy may find cracks but does so less comprehensively. Thus, the suggested method is to use cross-section samples.

Acknowledgements

The authors are grateful for the financial support provided by Business Finland Oy (former Tekes) in the form of research projects WIMMA Dnro 1566/31/2015 and MaNuMiES (Dnro 3361/31/2015) and Wärtsilä Finland Oy.

References

[1] Dobromirski JM. Variables of fretting process: are there 50 of them? In: Attia MH, Waterhouse RB, editors. Stand. Frett. Fatigue test methods equipment, ASTM STP 1159 Philadelphia: American Society for Testing and Materials; 1992. p. 60–6. https://doi.org/10.1520/STP1159-EB.

[2] Fouvry S, Kapsa P, Vincent L. Quantification of fretting damage. Wear 1996;200:186–205. https://doi.org/10.1016/S0043-1648(96)07306-1.

[3] Vingsbo O, Söderberg S. On fretting maps. Wear 1988;126:131–47. https://doi.org/10.1016/0043-1648(88)90134-2.

[4] Zhou ZR, Vincent L. Mixed fretting regime. Wear 1995;181–183:531–6. https://doi.org/10.1016/0043-1648(95)90168-X.

[5] Hintikka J, Lehtovaara A, Mäntylä A. Fretting-induced friction and wear in large flat-on-flat contact with quenched and tempered steel. Tribol Int 2015;92:191–202. https://doi.org/10.1016/j.triboint.2015.06.008.

[6] Leidich E, Maiwald A, Vidner J. A proposal for a fretting wear criterion for coated systems with complete contact based on accumulated friction energy density. Wear 2013;297:903–10. https://doi.org/10.1016/j.wear.2012.11.006.

[7] Vadivuchezhian K, Sundar S, Murthy H. Effect of variable friction coefficient on contact tractions. Tribol Int 2011;44:1433–42. https://doi.org/10.1016/j.triboint.2011.03.022.

[8] Waterhouse RB. Fretting fatigue. London: Applied Science Publishers; 1981.

[9] Cortez R, Mall S, Calcaterra JR. Investigation of variable amplitude loading on fretting fatigue behavior of Ti–6Al–4V. Int J Fatigue 1999;21:709–17. https://doi.org/10.1016/S0142-1123(99)00034-1.

[10] Conner BP, Hutson AL, Chambon L. Observations of fretting fatigue micro-damage of Ti-6Al-4V. Wear 2003;255:259–68. https://doi.org/10.1016/S0043-1648(03)00152-2.

[11] Antoniou RA, Radtke TC. Mechanisms of fretting-fatigue of titanium alloys. Mater Sci Eng 1997;237:229–40. https://doi.org/10.1016/S0921-5093(97)00419-X.

[12] Pape JA, Neu RW. Subsurface damage development during fretting fatigue of high strength steel. Tribol Int 2007;40:1111–9. https://doi.org/10.1016/j.triboint.2006.10.009.

[13] Wallace JM, Neu RW. Fretting fatigue crack nucleation in Ti-6Al-4V. Fatigue Fract Eng Mater Struct 2003;26:199–214. https://doi.org/10.1046/j.1460-2695.2003.00553.x.

[14] Swalla DR, Neu RW, McDowell DL. Microstructural characterization of Ti-6Al-4V subjected to fretting. J Tribol 2004;126:809–16. https://doi.org/10.1115/1.1792677.

[15] Xin L, Wang ZH, Li J, Lu Y, Shoji T. Microstructural characterization of subsurface caused by fretting wear of Inconel 690TT alloy. Mater Charact 2016;115:32–8. https://doi.org/10.1016/j.matchar.2016.03.010.

[16] Pape JA, Neu RW. Fretting fatigue damage accumulation in PH13 – 8Mo stainless steel. Int J Fatigue 2001;23:437–44. https://doi.org/10.1016/S0142-1123(01)00140-2.

[17] Szolwinski MP, Farris TN. Observation, analysis and prediction of fretting fatigue in 2024–T351 aluminum alloy. Wear 1998;221:24–36. https://doi.org/10.1016/S0043-1648(98)00264-6.

[18] Bertini L, Santus C. Fretting fatigue tests on shrink-fit specimens and investigations into the strength enhancement induced by deep rolling. Int J Fatigue 2015;81:179–90. https://doi.org/10.1016/j.ijfatigue.2015.08.007.

[19] Holopainen S, Juoksukangas J, Kouhia R, Lehtovaara A, Saksala T. An investigation of fatigue damage development under complete contact fretting test conditions. J Struct Mech 2016;49:151–9.

[20] Vázquez J, Navarro C, Domínguez J. Analysis of fretting fatigue initial crack path in Al7075-T651 using cylindrical contact. Tribol Int 2017;108:87–94. https://doi.org/10.1016/j.triboint.2016.09.023.

[21] Waterhouse RB, Taylor DE. The initiation of fatigue cracks in a 0.7% carbon steel by fretting. Wear 1971;17:139–47. https://doi.org/10.1016/0043-1648(71)90024-X.

[22] Xin L, Luo H, Han J, Lu Y, Shoji T. Damage mechanism of Alloy 690TT mated with Type 304 stainless steel during fretting wear in partial slip regime. Mater Charact 2017;132:284–92. https://doi.org/10.1016/j.matchar.2017.08.024.

[23] Waterhouse RB. Fretting Corrosion. Oxford: Pergamon press; 1972.

[24] Namjoshi SA, Mall S, Jain VK, Jin O. Fretting fatigue crack initiation mechanism in Ti-6Al-4V. Fatigue Fract Eng Mater Struct 2002;25:955–64. https://doi.org/10.1046/j.1460-2695.2002.00549.x.

[25] Juoksukangas J, Lehtovaara A, Mäntylä A. Development of a complete contact fretting test device. Proc Inst Mech Eng Part J J Eng Tribol 2013;227:570–8. https://doi.org/10.1177/1350650112466162.

[26] Juoksukangas J, Lehtovaara A, Mäntylä A. The effect of contact edge geometry on fretting fatigue behavior in complete contacts. Wear 2013;308:206–12. https://doi.org/10.1016/j.wear.2013.06.013.

[27] Juoksukangas J, Lehtovaara A, Mäntylä A. Effect of contact pressure on fretting fatigue life in complete contacts. Proc seventh int symp frett fatigue (ISFF7). UK: Oxford Univ. Oxford; 2013. p. 2.

[28] Juoksukangas J, Lehtovaara A, Mäntylä A. Experimental and numerical investigation of fretting fatigue behavior in bolted joints. Tribol Int 2016;103:440–8. https://doi.org/10.1016/j.triboint.2016.07.021.

[29] Hintikka J, Lehtovaara A, Mäntylä A. Normal displacements in non-Coulomb friction conditions during fretting. Tribol Int 2016;94:633–9. https://doi.org/10.1016/j.triboint.2015.10.029.

[30] Hintikka J, Juoksukangas J, Lehtovaara A, Frondelius T, Mäntylä A. Non-idealities in fretting contacts. J Struct Mech 2017;50:171–4. https://doi.org/10.23998/rm.64886.

[31] Nowell D, Dini D, Hills DA. Recent developments in the understanding of fretting fatigue. Eng Fract Mech 2006;73:207–22. https://doi.org/10.1016/j.engfracmech.2005.01.013.

[32] Araújo JA, Nowell D, Vivacqua RC. The use of multiaxial fatigue models to predict fretting fatigue life of components subjected to different contact stress fields. Fatigue Fract Eng Mater Struct 2004;27:967–78. https://doi.org/10.1111/j.1460-2695.2004.00820.x.

[33] Navarro C, Muñoz S, Domínguez J. On the use of multiaxial fatigue criteria for fretting fatigue life assessment. Int J Fatigue 2008;30:32–44. https://doi.org/10.1016/j.ijfatigue.2007.02.018.

[34] Mäntylä A, Göös J, Leppänen A, Frondelius T. Large bore engine connecting rod fretting analysis. J Struct Mech 2017;50:239–43. https://doi.org/10.23998/rm.64914.

[35] Niva J. An examination of the propagation of fretting cracks using fracture mechanics. J Struct Mech 2017;50:186–90. https://doi.org/10.23998/rm.64935. (in Finnish).

[36] Nurmi V, Hintikka J, Juoksukangas J, Honkanen M, Vippola M, Lehtovaara A, Mäntylä A, Vaara J, Frondelius T. The formation and characterization of fretting-induced degradation layers using quenched and tempered steel. Tribol Int 2019;131:258–67. https://doi.org/10.1016/j.triboint.2018.09.012.

[37] Hintikka J, Mäntylä A, Vaara J, Frondelius T, Lehtovaara A. Stable and unstable friction in fretting contacts. Tribol Int 2019;131:73–82. https://doi.org/10.1016/j.triboint.2018.10.014.

[38] Hintikka J, Lehtovaara A, Frondelius T, Mäntylä A. Tangential traction instability in fretting contact below fully developed friction load. J Struct Mech 2017;50:175–8. https://doi.org/10.23998/rm.65105.

[39] Jeung HK, Kwon JD, Lee CY. Crack initiation and propagation under fretting fatigue of inconel 600 alloy. J Mech Sci Technol 2015;29:5241–4. https://doi.org/10.1007/s12206-015-1124-8.

[40] Pape JA, Neu RW. A comparative study of the fretting fatigue behavior of 4340 steel and PH 13–8 Mo stainless steel. Int J Fatigue 2007;29:2219–29. https://doi.org/10.1016/j.ijfatigue.2006.12.016.